

## Electrochemical biosensors for on-chip detection of oxidative stress from immune cells

Jun Yan,<sup>1</sup> Valber A. Pedrosa,<sup>2</sup> James Enomoto,<sup>1</sup> Aleksandr L. Simonian,<sup>2</sup> and Alexander Revzin<sup>1,a)</sup>

<sup>1</sup>*Department of Biomedical Engineering, University of California, Davis, 451 East Health Sciences St. #2619, Davis, California 95616, USA*

<sup>2</sup>*Department of Materials Engineering, Auburn University, Auburn, Alabama 36849, USA*

(Received 25 January 2011; accepted 19 July 2011; published online 20 September 2011)

Seamless integration of biological components with electrochemical sensors is critical in the development of microdevices for cell analysis. The present paper describes the integration miniature Au electrodes next to immune cells (macrophages) in order to detect cell-secreted hydrogen peroxide ( $\text{H}_2\text{O}_2$ ). Photopatterning of poly(ethylene glycol) (PEG) hydrogels was used to both immobilize horseradish peroxidase molecules onto electrodes and to define regions for cell attachment in the vicinity of sensing electrodes. Electrodes micropatterned in such a manner were enclosed inside poly(dimethylsiloxane) fluid conduits and incubated with macrophages. The cells attached onto the exposed glass regions in the vicinity of the electrodes and nowhere else on the non-fouling PEG hydrogel surface. A microfluidic device was converted into an electrochemical cell by placing flow-through Ag/AgCl reference and Pt wire counter electrodes at the outlet and inlet, respectively. This microdevice with integrated  $\text{H}_2\text{O}_2$ -sensing electrodes had sensitivity of  $27 \mu\text{A}/\text{cm}^2 \text{ mM}$  with a limit of detection of  $2 \mu\text{M}$ . Importantly, this microdevice allowed controllable seeding of macrophages next to electrodes, activation of these cells and on-chip monitoring of  $\text{H}_2\text{O}_2$  release in real time. In the future, this biosensor platform may be utilized for monitoring of macrophage responses to pathogens or for the study of inflammatory signaling in micropatterned cell cultures. © 2011 American Institute of Physics. [doi:10.1063/1.3624739]

### INTRODUCTION

Inflammatory processes play an important role in a number of pathologies including diabetes,<sup>1</sup> cancer,<sup>2</sup> and tissue fibrosis.<sup>3</sup> Molecules released by immune cells during inflammation are critical in combating pathogens. Macrophages are immune cells that reside in the tissue and are first to respond to invading pathogens. These cells have produce an array of inflammatory markers including cytokines and reactive oxygen species (ROS).<sup>4</sup> ROS is a collective term that refers to chemical species formed by incomplete reduction of oxygen, including superoxide anion ( $\text{O}_2^{\cdot-}$ ), hydrogen peroxide ( $\text{H}_2\text{O}_2$ ), and hydroxyl radical ( $\text{OH}\cdot$ ).<sup>5</sup> ROS compounds such as superoxide anion ( $\text{O}_2^{\cdot-}$ ) are unstable and, upon degradation, form a more stable  $\text{H}_2\text{O}_2$  compound. ROS molecules are released by macrophages and other immune cells to eliminate pathogens and cleanse site of the injury. Therefore, appearance of ROS is an important indicator of inflammation and may serve as a diagnostic marker of the immune system interaction with pathogens.

Bioanalytical approaches for detection of  $\text{H}_2\text{O}_2$  described in the literature include chemiluminescence,<sup>6</sup> fluorescence,<sup>7</sup> and electrochemistry.<sup>8,9</sup> The latter approach is particularly attractive due to simplicity and reliability of measurements, and the possibility for miniaturization. Electrochemical biosensors commonly rely on the enzyme, horseradish peroxidase (HRP)—an oxidoreductase enzyme that catalyzes reduction of  $\text{H}_2\text{O}_2$ . This reduction can be detected at the electrode either directly,<sup>10,11</sup> or through redox mediators such as ferrocene- and osmium-based

<sup>a)</sup> Author to whom correspondence should be addressed. Electronic mail: arevzin@ucdavis.edu.

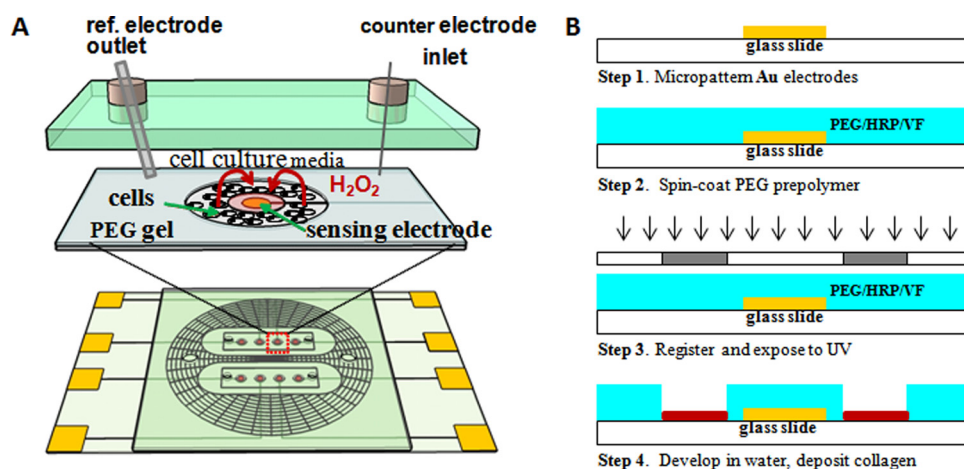


FIG. 1. (a) Upper panel: schematic of a single electrode for detection of cell secreted  $\text{H}_2\text{O}_2$ . Macrophages are captured on a micropatterned surface in the vicinity of sensing electrode. The sensor consists of an HRP-carrying hydrogel disc immobilized on top of  $300\ \mu\text{m}$  diameter Au electrode. Each channel constituted an electrochemical cell with Ag/AgCl flow-through reference and Pt wire counter electrodes placed at the outlet and inlet, respectively. Lower panel: There were two parallel microfluidic channels in the device, with 4 individually addressable electrodes in each microfluidic channel. Each fluidic channel had a volume of  $3\ \mu\text{l}$ . (B) Step-by-step diagram for immobilizing HRP carrying hydrogel microstructures on top of Au electrodes.

redox polymers.<sup>12–14</sup> Electrochemistry has also become a powerful tool for monitoring electroactive metabolites secreted or taken up by living cells.<sup>15–19</sup> In terms of monitoring of oxidative stress, there have been several reports of electrochemical biosensors for the detection of nitric oxide secreted from cells<sup>20–22</sup> and a recent report describing  $\text{H}_2\text{O}_2$  release from leukocytes.<sup>13</sup> However, several technical challenges cell sensing remain unaddressed, including: (1) how to position cells near the sensing electrodes and (2) how to ensure that, while reporting on cell function, these electrodes remain non-fouling and unaffected by cellular activity.

The goal of this paper was to develop a biomaterial micropatterning strategy to enable reproducible placement of macrophages in the proximity of  $\text{H}_2\text{O}_2$  biosensors and to ensure that the sensing electrodes were not fouled. To achieve this, we utilized poly(ethylene glycol) (PEG) hydrogel photolithography—an approach employed by us previously to design cell-surface interactions.<sup>23–25</sup> In addition to preventing cell attachment, PEG hydrogels provide an excellent matrix for entrapment of enzymes<sup>26–28</sup> and also prevent electrode fouling.<sup>29,30</sup> Recently, we demonstrated the use of PEG hydrogel micropatterning for fabricating enzyme-based electrodes for detection of glucose and lactate.<sup>28</sup>

In the present study, the enzyme-electrode fabrication process was modified to include sites for cell attachment next to enzyme electrodes (Figure 1). A micropatterned cell culture/biosensor surface was incorporated into a two-channel microfluidic device with flow-through reference (Ag/AgCl) and counter (Pt) electrodes. This microdevice was used to seed, culture, activate macrophages, and monitor dynamics of  $\text{H}_2\text{O}_2$  release from these cells. Microfluidic chambers allowed us to decrease the volume of electrochemical cell to  $3\ \mu\text{l}$  and to control delivery of stimulants to cells. In the future, we envision placing biosensors for several analytes next to cells for multi-parametric analysis of cell function. Microfluidic devices with integrated biosensors will also be useful for cell cultivation with on-chip monitoring of cell function.

## MATERIALS AND METHODS

### Materials

Poly (ethylene glycol) diacrylate (PEG-DA, MW 575), 2-hydroxy-2-methyl-propiophenone (photoinitiator), 99.9% toluene,  $\text{H}_2\text{O}_2$ , PMA (Phorbol 12-myristate 13-acetate), and HRP were

purchased from Sigma (St Louis, MO, USA). Chromium etchant (CR-4S) and gold etchant (Au-5) were from Cyantek Corporation (Fremont, CA). Positive photoresist (S1813) and its developer solution (MF-319) were brought from Shipley (Marlborough, MA). 3-Acryloxypropyl trichlorosilane was from Gelest, Inc. (Morrisville, PA). Phosphate buffered saline (PBS, 0.1 M, pH 7.4) without calcium and magnesium was from Fisher Scientific and used to prepare aqueous solution. Poly(dimethylsiloxane) (PDMS) and its curing agents were purchased from Dow Corning (Midland, MI). J774 Macrophages cell line was purchased from American Type Culture Collection (ATCC). Alexa546-Streptavidin was obtained from Invitrogen (Carlsbad, CA).

### Fabrication of Au electrode arrays

The layout of electrode array was prepared in AutoCAD, converted into plastic transparencies by CAD Art Services (Portland, OR) and then transferred onto quartz/chrome plates using standard microfabrication approaches. The fabrication of gold electrodes has been described in our previous reports.<sup>28,31</sup> Briefly, standard (75 mm × 25 mm) glass slides were sputter-coated with 15 nm Cr adhesion layer and 100 nm Au layer by Lance Goddard Associates (Santa Clara, CA). Positive photoresist was micropatterned on top of Au/Cr and used as a protective layer during wet etching of the metal. As shown in Figure 1(a) (lower panel), resulting Au micropatterns consisted of eight electrodes connected by leads to contact pads for individual addressability. Each Au electrode was 300 μm in diameter with 16 μm wide lead and 2 mm × 2 mm square contact pad. After wet etching, the photoresist layer was retained on top of the Au pattern and was used as a protective layer during silanization procedure described below. If left unprotected, Au regions became irreversibly insulated by the silane layer.

### Integration of enzyme-containing hydrogel microstructures with Au electrodes

The glass substrates with photoresist-covered Au electrodes were modified with acrylated silane according to the protocol described by us previously.<sup>31</sup> This step was necessary to ensure anchoring of hydrogel structures onto glass substrates. After the silane modification step, substrates were sonicated in acetone for 2 min to remove the photoresist and then placed in an oven for 3 h at 100 °C to crosslink the silane layer.

When preparing enzyme electrodes, HRP was dissolved in PBS buffer (pH 6.0) to reach the concentration of 10 mg/ml. In addition, glutaraldehyde was added to the enzyme solution at 2% (v/v) to improve enzyme retention. In parallel, the prepolymer solution was prepared by adding 2% (v/v) photoinitiator (2-hydroxy-2-methyl-propiophenone) to 1 ml of pure PEG-diacrylate (DA) (MW 575). The HRP-PEG hydrogel prepolymer solutions were prepared by adding 5 μL, 10 μL, 20 μL, and 40 μL of the enzyme solution mixed with glutaraldehyde into 50 μL of PEG-DA. Therefore, four different volumetric ratios of HRP:PEG were prepared: 1:10, 1:5, 2:5, and 4:5. The mixture was stirred for 4 h at 4 °C to better distribute enzyme molecules in the prepolymer.

The procedure for patterning hydrogel microstructures on electrodes is described schematically in Figure 1(b). PEG-based prepolymer solution was spin-coated at 800 rpm for 4 s onto glass slides containing Au electrode patterns. A photomask was registered with an electrode pattern and then exposed to UV light at 65 mW/cm<sup>2</sup> for 10 s using Omnicare 1000 light source (EXFO, Mississauga, Ontario, Canada) to convert liquid prepolymer into cross-linked hydrogel. The surfaces were developed in de-ionized (DI) water for 3 min to remove unpolymerized PEG precursor solution. Enzyme carrying hydrogel microstructures were made larger than Au electrodes—600 μm and 300 μm diameter for hydrogel and Au features, respectively. This was done to ensure that hydrogel elements attached to the silanized glass regions of the substrate.

Sites for cell attachment were created by micropatterning a second hydrogel layer in registration with hydrogel/Au electrodes. This second gel layer did not carry HRP molecules and was used to define 300 μm wide annular cell adhesive regions on the glass surface. The micropatterned glass surfaces were incubated with collagen (I) (0.2 mg/ml) for 30 min to promote attachment of macrophages to glass (see Figure 3). To visualize immobilization of protein

molecules in the regions designated for cell attachment, micropatterned surfaces were incubated with avidin-Alexa546 conjugate and imaged using fluorescence microscopy.

### **Fabrication of microfluidic devices for detection of cell-secreted H<sub>2</sub>O<sub>2</sub>**

Electrode-containing micropatterned surfaces were outfitted with microfluidic conduits in order to control delivery of cells and activating reagents, and to carry out electrochemical experiments in a small volume (see Figure 1(a) lower panel for device layout). Poly(dimethylsiloxane) (PDMS)-based microfluidic devices were fabricated using standard soft lithography methods. The design of these devices was described in detail in our previous publication.<sup>32</sup> Briefly, a microfluidic device contained two working chambers with width-length-height dimensions of  $6 \times 10 \times 0.1$  mm (volume  $3 \mu\text{l}$ ). Inlet and outlet for these chambers were punched with a blunt 16 gauge needle. A PDMS layer also included a web of auxiliary channels that had no communication with the working channels and had a separate inlet/outlet. These auxiliary channels were used to apply negative pressure and to suction the PDMS onto micropatterned glass substrates. The pressure-driven flow was generated by a precision syringe pump (Harvard Apparatus, Boston, MA). All the electrochemical experiments described in this paper were done inside a microfluidic device.

In these experiments, a flow-through Ag/AgCl reference electrode was positioned at the outlet of the fluidic device and connected to a syringe pump. A blunt 20 gauge needle carrying a plastic hub with volume of  $100 \mu\text{l}$  was inserted in the inlet. The Pt counter electrode was placed inside the hub. Enzyme-carrying hydrogel/Au electrodes were located inside the fluidic channels and served as working electrodes. Therefore, each fluidic chamber constituted a three-electrode electrochemical cell. All electrochemistry experiments were performed using a CH Instruments (CH1820B) bipotentiostat.

### **Calibration of H<sub>2</sub>O<sub>2</sub> biosensor**

Prior to detecting cell-secreted H<sub>2</sub>O<sub>2</sub>, performance of enzyme-electrodes was characterized using known analyte concentrations. To detect H<sub>2</sub>O<sub>2</sub>, hydrogel/Au electrodes were poised at  $-0.2$  V (vs. Ag/AgCl) and then exposed to aliquots of H<sub>2</sub>O<sub>2</sub> ranging from 0.02 to 2 mM. In these experiments,  $40 \mu\text{l}$  of a given H<sub>2</sub>O<sub>2</sub> concentration was infused into a fluidic chamber. Current vs. time response of the biosensor was recorded under static conditions (no flow). Subsequently, microfluidic device was disassembled, extensively washed with PBS, reassembled and infused with a different (higher) concentration of analyte.

### **Detecting H<sub>2</sub>O<sub>2</sub> release by activated macrophages**

Mouse macrophage cells (J774A) were cultured at  $37^\circ\text{C}$  with 5% CO<sub>2</sub> in phenol red-free Dulbecco's Modified Eagle's Medium (DMEM) supplemented with 10% fetal bovine serum (FBS). These cells were grown in suspension culture in 50 ml bioreactor tubes (Techno Plastic Products) on a rolling apparatus (Stovall). The cells were passaged two times a week by centrifuging and re-suspending in fresh culture media.

Prior to cell seeding, 1 ml cell suspension was concentrated by centrifugation and was resuspended in DMEM at  $\sim 15 \times 10^6$  cells/ml. Cell seeding and washing steps were carried out in the microfluidic device.  $50 \mu\text{l}$  of cell solution was placed in the inlet and introduced into the microfluidic channel by pulling the syringe at the flow rate of  $10 \mu\text{l}/\text{min}$ . Flow was stopped once cells filled the channel. After 30 min incubation,  $1 \times$  PBS was injected into the channel at a flow rate of  $50 \mu\text{l}/\text{min}$  to wash away unbound cells. DMEM with  $100 \mu\text{g}/\text{ml}$  of PMA was also delivered into the microfluidic channels to induce mitogenic activation of macrophages. Release of H<sub>2</sub>O<sub>2</sub> from activated macrophages was monitored using amperometry over the course of  $\sim 3$  h. Electrochemical monitoring of H<sub>2</sub>O<sub>2</sub> secretion from macrophages began 40 min before stimulation with PMA and continued for additional 140 min in the presence of the stimulant. The flow was stopped during electrochemical measurements of cell-secreted H<sub>2</sub>O<sub>2</sub> in order to eliminate convection and help pre-concentrate secreted analytes in the vicinity

of the cells and electrodes. Controls for these experiments included monitoring of cells without PMA activation as well as challenging peroxide-sensing electrodes with PMA in culture media without cells. These controls were designed to prove that unstimulated macrophages did not release appreciable amounts of  $\text{H}_2\text{O}_2$  and that PMA or components of the culture media did not interfere with electrochemical detection of  $\text{H}_2\text{O}_2$ .

To better characterize dynamics of  $\text{H}_2\text{O}_2$  production in macrophages we monitored intracellular ROS using a reported molecule 2'-7'-dichlorodihydrofluorescein diacetate (DCFH-DA). In these experiments, J774 macrophages were seeded into 6-well plates and incubated with 5  $\mu\text{M}$  DCFH-DA in phenol-red free DMEM for 30 min at 37°. Subsequently, cells were washed extensive in PBS to remove DCFH-DA that did not penetrate the cells. The macrophages were stimulated by adding PMA into DMEM to create 1  $\mu\text{g}/\text{ml}$  concentration. Fluorescence was measured every 10 min for 2 h post stimulation using plate reader (Tecan) employing excitation/emission of 490 nm/530 nm. Plates were stored in a tissue culture incubator between measurements.

## RESULTS AND DISCUSSIONS

In this study, we leveraged dual functionality of PEG hydrogel—as both a non-fouling surface and a matrix for enzyme entrapment—to micropattern cell attachment sites next to enzyme-based electrodes. Micropatterned surfaces were enclosed inside a microfluidic device to create an electrochemical cell with a small ( $\sim 3 \mu\text{l}$ ) volume. The design of the biointerface allowed us to reproducibly position small groups of cells in the proximity of HRP-containing electrodes and to monitor real-time  $\text{H}_2\text{O}_2$  release from activated macrophages.

### Fabrication of hydrogel/Au electrodes

Our device consisted of an array of  $2 \times 4$  Au electrodes fabricated so as to position 4 electrodes inside each channel of a two-chamber microfluidic device (see lower panel of Figure 1(a)). The second channel of the fluidic device provided either a negative control (cells receiving no stimulation) or was used to expose cells to a different stimulant. PEG hydrogel photolithography was used to convert Au micropatterns into enzyme-based electrodes. This hydrogel micropatterning technique is similar to traditional photoresist lithography as it involves the same spin-coating, alignment, exposure, and development steps. Using this process, enzyme-containing hydrogel disks (600  $\mu\text{m}$  diameter) were fabricated directly on top of circular 300  $\mu\text{m}$  diameter Au electrodes. Importantly, photomasks were designed such as to fabricate moats (300  $\mu\text{m}$  wide) in the gel layer (see Figures 2(a) and 2(b) for images of electrodes and hydrogel patterns). Because PEG gel is non-fouling, immune cells were expected to attach on the glass surface at the bottom of each moat in the immediate vicinity of HRP-based electrochemical biosensors.

Micropatterned surfaces shown in Figure 3(b) were incubated with cell-adhesive ligands (collagen I) or fibronectin) to promote macrophage attachment to these regions. As a proof of concept, Figure 2(c) shows selective adsorption of fluorescently labeled protein molecules on the annular region of glass that was left unprotected during hydrogel fabrication process. This highlights our ability to define sites of protein attachment on the micropatterned sensing surface.

### Optimizing performance of $\text{H}_2\text{O}_2$ -sensing electrodes

After fabricating enzyme-based hydrogel/Au electrodes and outfitting these electrodes with microfluidic channels, we characterized the response of these microdevices to known concentrations of  $\text{H}_2\text{O}_2$ . It should be noted that  $\text{H}_2\text{O}_2$  can be reduced or oxidized at negatively or positively poised electrodes. Given the oxidation of interfering substances such as ascorbic acid and uric acid at potentials exceeding 0.4 V vs. Ag/AgCl reference,<sup>33</sup> detection of peroxide is commonly carried out at reductive (negative potentials) according to the reaction presented below<sup>34,35</sup>

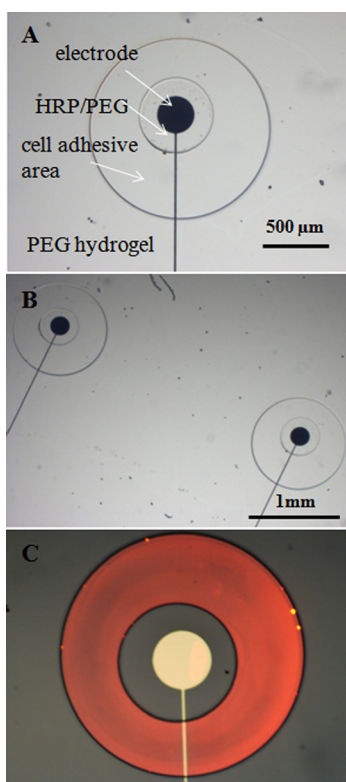


FIG. 2. (a and b) Au electrodes ( $300\ \mu\text{m}$  diameter) integrated with hydrogel microstructures ( $600\ \mu\text{m}$  diameter). A  $300\ \mu\text{m}$  wide ring around each electrode served as a site for cell attachment. (c) Brightfield/fluorescence overlay image showing fluorescently labeled protein (avidin-Alexa546 (red)) deposited in the site of cell attachment. This picture highlights that hydrogel structures were non-fouling and that proteins adsorbed only on the exposed glass regions. This micropatterning strategy was used to reproducibly position cells next to electrodes.



While the reduction reaction may occur in the absence of HRP, immobilizing enzyme molecules on the electrode dramatically improves sensitivity of the biosensor. As discussed later in this paper, we observe 60 fold signal enhancement with HRP-containing electrodes compared to electrodes without HRP. This enzyme catalyzes the reduction reaction shown above by donating electrons (from the iron-containing heme cofactor) and becoming oxidized in the process.<sup>36</sup> In nonelectrochemical HRP-based assays, a substrate is used to help revert enzyme molecules into reduced state. The biosensor described here relies on direct electron transfer from the electrode to HRP to revert the enzyme into active form. The reductive currents appear at a negatively poised electrode when HRP catalyzes breakdown of  $\text{H}_2\text{O}_2$ .

Prior to carrying out cell detection experiments, we wanted to optimize performance of the biosensor. Specifically, we characterized the dependence of sensor responses on HRP loading into the hydrogel and on the working potential. PEG prepolymer formulations with varying amounts of HRP were prepared to create 1:10, 1:5, 2:5, and 4:5 volumetric ratio of HRP:PEG solution. Hydrogel-coated Au electrodes were poised at  $-0.2\ \text{V}$  vs. Ag/AgCl reference and challenged with  $200\ \mu\text{M}$   $\text{H}_2\text{O}_2$ . As shown in Figure 3(a), the sensitivity of the hydrogel-coated electrodes was dependent on the enzyme loading. Hydrogels created with higher HRP to PEG ratios provided stronger response to  $200\ \mu\text{M}$   $\text{H}_2\text{O}_2$ , with hydrogel/Au electrodes based on 4:5 HRP:PEG ratio providing the highest reductive current. Please note that enzyme loading ratios above 4:5 (v/v) led to problems with gelation of the prepolymer and therefore could not be used in our experiments. Based on these results, biosensors used in all subsequent experiments were prepared using 4:5 (v/v) ratio of HRP to PEG.

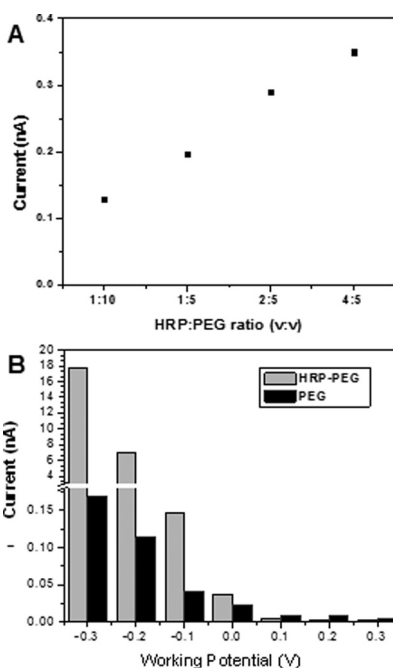


FIG. 3. (a) The effect of HRP loading on the biosensor response. Ratios represent v/v of HRP in PEG prepolymer solutions. Hydrogel-coated Au electrodes were poised at  $-0.2\text{V}$  vs. Ag/AgCl references and were challenged with  $200\ \mu\text{M}$   $\text{H}_2\text{O}_2$ . Amperometric responses from different electrode formulations were normalized by the response from a 1:10 HRP:PEG hydrogel coating. (b) Electrical responses of electrodes to  $200\ \mu\text{M}$   $\text{H}_2\text{O}_2$  at working potentials ranging from  $-0.3$  to  $0.6\ \text{V}$  vs. Ag/AgCl reference. Electrodes coated with HRP-PEG were compared to electrodes covered with PEG hydrogel only.

We also investigated the optimal reduction potential for performing  $\text{H}_2\text{O}_2$  detection. In these experiments, hydrogel/Au electrodes with and without HRP were poised at potentials ranging from  $-0.3$  to  $0.3\text{V}$  vs. Ag/AgCl and were challenged with  $200\ \mu\text{M}$  of  $\text{H}_2\text{O}_2$ . Figure 3(b) reveals several insights into signal vs. applied potential relationship: (1) hydrogel modified electrodes exhibited higher current density at reductive (negative) voltages, (2) HRP-containing hydrogel/Au electrodes were  $\sim 60$  times more sensitive to  $\text{H}_2\text{O}_2$  compared to gel-coated electrodes without enzyme at working potential  $-0.2\ \text{V}$ , and (3) the presence of HRP in the hydrogel did not contribute to improved sensitivity at oxidative (positive) potentials. Based on these observations, we chose to employ HRP-modified hydrogel/Au electrodes at  $-0.2\ \text{V}$  vs. Ag/AgCl reference. While electrodes poised at more negative potentials were more sensitive, we chose to operate our biosensors at  $-0.2\text{V}$  to avoid interference due to the reduction of oxygen that is known to occur at more negative potentials.<sup>37</sup>

### Calibrating $\text{H}_2\text{O}_2$ biosensors

We proceeded to characterize the response of the hydrogel/Au electrodes to known concentrations of  $\text{H}_2\text{O}_2$ . All experiments were carried out inside microfluidic devices (see lower panel of Figure 1(a)). The changes in cathodic (reductive) current were observed upon infusion of varying  $\text{H}_2\text{O}_2$  concentrations into the microfluidic chamber. Figures 4(a) and 4(b) show typical responses of biosensors to challenges with known concentration of analyte. These amperometry experiments show the response time of the biosensor—defined as the time to reach 90% of signal—to be  $\sim 10\ \text{s}$ . Sensor responses to predefined  $\text{H}_2\text{O}_2$  concentration were used to construct calibration curve shown in Figure 4(c). This calibration curve shows a linear response of HRP/hydrogel/Au sensing electrodes from  $2\ \mu\text{M}$  to  $500\ \mu\text{M}$   $\text{H}_2\text{O}_2$  with an  $R^2$  value of 0.96. The  $\text{H}_2\text{O}_2$  biosensor had sensitivity of  $27\ \mu\text{A}/\text{mM}\cdot\text{cm}^2$  and the detection limit of  $\sim 2\ \mu\text{M}$ . The linear range of our biosensor extended up to  $2\ \text{mM}$  (data not shown); however, given that cells

were expected to release relatively low amounts of  $\text{H}_2\text{O}_2$ , we chose to present a lower concentration range of this analyte.

### Detecting $\text{H}_2\text{O}_2$ release from activated macrophages

After validating biosensor response in a cell-free system, we wanted to monitor endogenous  $\text{H}_2\text{O}_2$  production by macrophages. Macrophages are important immune cells that actively participate in inflammatory processes by secreting cytokines and ROS.<sup>4</sup> Our eventual goal is to employ microdevices for profiling oxidative burst and cytokine production in macrophages isolated from clinical samples. The goal of the present study was to demonstrate the utility of our microdevice for the detection of cell-secreted  $\text{H}_2\text{O}_2$ . For this purpose, we used a mouse macrophage cell line (J774) that could be mitogenically activated with PMA to induce  $\text{H}_2\text{O}_2$  release. Cells that did not receive PMA stimulation were used as a negative control in our experiments. The ability to control cell attachment in relation to the sensing element is an important feature of our biosensor platform. The use of a micropatterned, non-fouling hydrogel layer has the following advantages: (1) cells were not attaching on top of the electrodes and were not interfering with electrochemical measurements, (2) cells could be reproducibly positioned in the proximity of electrodes in order to detect non-steady state metabolite fluxes, this would be particularly useful when dealing with clinical samples that may not have a lot of cells, and (3) attachment sites next to the electrodes may be modified in the future to capture monocytes/macrophages or other cell types from a heterogeneous clinical sample (e.g., blood). Figure 5(a) shows representative image obtained after seeding macrophages on the micropatterned hydrogel/electrode surfaces. As seen from this image, cells with DAPI (blue)-stained nuclei attached in ring-shaped glass region formed within PEG hydrogel. Enzyme-carrying hydrogel disks formed on top of Au electrodes did not support cell attachment and remained non-fouling for the duration of experiments.

Figure 5(b) shows representative sensograms collected in our devices under different stimulation conditions. As shown in the upper sensogram, stimulation of macrophages with PMA led to appearance of reductive (negative) current that is associated with HRP-catalyzed breakdown of  $\text{H}_2\text{O}_2$  molecules. The maximum signal (net current change 8 pA) was observed after 60 min of PMA stimulation, after which the signal became weaker over the course of next 60 min. The  $\text{H}_2\text{O}_2$  secretion from  $\sim 1000$  macrophages under PMA stimulation was  $10.3 \pm 1.53 \mu\text{M}$  ( $n = 3$ ).

As demonstrated in Figures 4(a) and 4(b), our sensors show fast response to predefined concentrations of analyte, reaching 90% of maximal signal after  $\sim 10$  s, yet when tested with macrophages signal changes over the course of 60 to 90 min. It is therefore highly likely that dynamics of sensor response are defined by cellular activity as opposed to mass transport of analyte to the biosensor. To further corroborate this point, we tested intracellular production of  $\text{H}_2\text{O}_2$ ; reasoning that detection of analyte inside the cell would not be influenced by diffusion and would allow to focus solely on cellular activity. In these experiments, macrophages were incubated with peroxide-sensitive intracellular fluorophore dichlorodihydrofluorescein (DCFH) and activated with PMA as described above. These experiments (data not shown) revealed that intracellular ROS, as indicated by fluorescence signal, was increasing in activated macrophages over the course of 1 h, mimicking responses of extracellular electrochemical sensor. In addition to our own observations, there are published reports describing oxidative burst occurring on the time scale similar to that reported in this paper.<sup>38,39</sup>

Importantly, we carried out several control experiments to ensure that the signal observed in Figure 5(b) was indeed due to cellular activity. These control experiments revealed that: (1) no signal was observed from macrophages cultured next to hydrogel/Au electrodes without stimulant PMA (middle sensogram Figure 5(b)) and (2) no signal was observed in cell-free devices that were infused with PMA dissolved in culture media (lower sensogram Figure 5(b)). Additional control experiment involved fabrication of gel-covered electrodes without HRP and was designed to test whether detection of cellular response required presence of peroxide-specific enzyme HRP. When macrophages were captured near the electrode lacking HRP and were stimulated with PMA, no reductive currents were detected and sensograms were similar to those



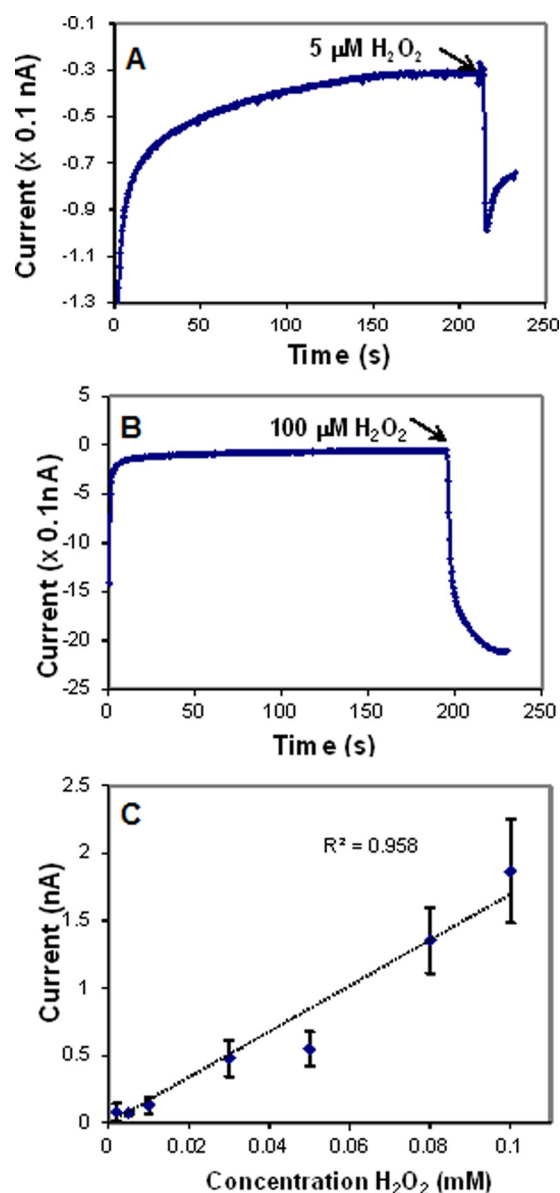


FIG. 4. (a and b) Amperometric responses of HRP/hydrogel/Au electrodes to 5  $\mu\text{M}$  and 100  $\mu\text{M}$   $\text{H}_2\text{O}_2$ . (b) Calibration curve of current vs. analyte concentration. HRP/hydrogel/Au electrodes showed sensitivity of  $27 \mu\text{A}/\text{mM}\cdot\text{cm}^2$  and the detection limit of  $\sim 2 \mu\text{M}$   $\text{H}_2\text{O}_2$ . In both sets of experiments electrodes were poised at  $-0.2 \text{ V}$  vs. Ag/AgCl.

shown in Figure 5(b). This control experiment further validated that the analyte produced by cells and detected at the sensing electrodes was indeed  $\text{H}_2\text{O}_2$ .

The findings described here are in line with our previous report of detecting extracellular  $\text{H}_2\text{O}_2$  using fluorescent (Amplex Red/HRP-based) hydrogel microstructures.<sup>39</sup> However, we found electrochemical biosensor to provide more robust, sensitive and reproducible results compared Amplex Red-based detection scheme. It should be noted that the  $\text{H}_2\text{O}_2$  production in macrophages measured in our paper is comparable to literature reports ( $0.03 \text{ nmol}/10^3 \text{ cells/h}$  in this paper vs.  $0.05\text{--}0.13 \text{ nmol}/10^3 \text{ cells/h}$  (Refs. 40–42)).

## CONCLUSIONS

In this paper, PEG hydrogel micropatterning was employed to both fabricate HRP-containing electrochemical biosensors and to define living cell/biosensor interface. These

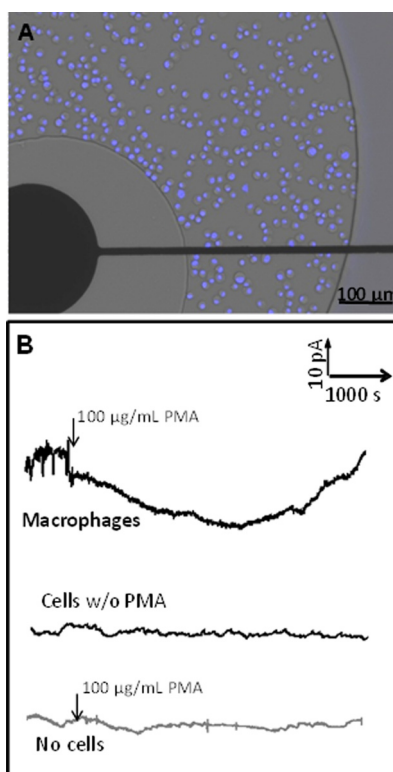


FIG. 5. (a) Macrophages attaching next to HRP-containing hydrogel/Au electrode. Cell nuclei are stained with 4',6-diamidino-2-phenylindole (DAPI) (blue color). (b) A smaller magnification image showing two electrodes integrated with cells. (c) Amperometric responses obtained from stimulated macrophages cultured next to sensing miniature electrodes. Measurements of electrode response to macrophages without stimulation and media with stimulant (PMA) but no cells were carried out in parallel, in the same device as cell detection experiment, and were used as controls. As seen from these negative current due to reduction of  $\text{H}_2\text{O}_2$  was only observed in the presence of activated macrophages. Electrodes were poised at  $-0.2$  V vs. Ag/AgCl.

micropatterned sensing/cell culture surfaces were integrated into a PDMS-based microfluidic device and outfitted with flow-through reference and counter electrodes. This way a microfluidic chamber served the purpose of a three-electrode electrochemical cell with HRP/hydrogel/Au electrodes serving as working electrodes. Macrophages injected into the microfluidic device and incubated with the surface, adhered on the glass regions around the HRP-coated electrodes. Importantly, the electrodes covered with PEG gel remained non-fouling and did not support cell attachment during cell seeding and analysis. Microdevices with integrated  $\text{H}_2\text{O}_2$ -sensing electrodes had sensitivity of  $27 \mu\text{A}/\text{cm}^2 \text{ mM}$  and lower limit of detection of  $2 \mu\text{M}$ . Importantly, this microdevice allowed real-time monitoring of extracellular  $\text{H}_2\text{O}_2$  produced by activated macrophages. We envision employing microdevices described here for monitoring oxidative burst in immune cells isolated from clinical samples. We also envision integrating electrochemical biosensors into micropatterned co-cultures<sup>24</sup> to simultaneously define and detect endocrine signaling between two distinct cell types.

## ACKNOWLEDGMENTS

The financial support for this study was provided by an NSF EFRI grant (0937997) and an NIH grant (CA126716) awarded to AR. ALS acknowledges working at the National Science Foundation during the time this study was carried out. The views expressed in this article are those of the authors and do not reflect the views of the National Science Foundation.

<sup>1</sup>R. Simmons, *Free Radic. Biol. Med.* **40**, 917 (2006).

<sup>2</sup>B. Halliwell, *Biochem. J.* **401**, 1 (2007).

- <sup>3</sup>A. Picardi, D. D'Avola, U. Vespasiani Gentilucci, G. Galati, E. Fiori, S. Spataro, and A. Afeltra, *Diabetes Metab. Res. Rev.* **22**, 274 (2006).
- <sup>4</sup>J. Kuby, *Immunology* (W.H. Freeman and Co., New York, 1998).
- <sup>5</sup>B. D'Autreaux and M. Toledano, *Nat. Rev. Mol. Cell Biol.* **8**, 813 (2007).
- <sup>6</sup>D. Lee, V. Erigala, M. Dasari, J. Yu, R. Dickson, and N. Murthy, *Int. J. Nanomed.* **3**, 471 (2008).
- <sup>7</sup>M. Zhou, Z. Diwu, N. Panchuk-Voloshina, and R. Haugland, *Anal. Biochem.* **253**, 162 (1997).
- <sup>8</sup>A. Lindgren, T. Ruzgas, L. Gorton, E. Csöregi, G. Ardila, I. Sakharov, and I. Gazaryan, *Biosens. Bioelectron.* **15**, 491 (2000).
- <sup>9</sup>S. R. Serradilla, B. R. Lopez, N. H. B. Mark, Jr., and J-M. Kauffmann, *Biosens. Bioelectron.* **17**, 921 (2002).
- <sup>10</sup>B. Munge, R. Dowd, C. Krause, and L. Millord, *Electroanalysis* **21**, 2241 (2009).
- <sup>11</sup>K. Yamamoto, G. Shi, T. Zhou, F. Xu, J. Xu, T. Kato, J-Y. Jin, and L. Jin, *Analyst* **128**, 249 (2003).
- <sup>12</sup>B. Chikkaveeraiah, H. Liu, V. Mani, F. Papadimitrakopoulos, and J. Rusling, *Electrochem. Commun.* **11**, 819 (2009).
- <sup>13</sup>K. Inoue, K. Ino, H. Shiku, S. Kasai, T. Yasukawa, F. Mizutani, and T. Matsue, *Biosens. Bioelectron.* **25**, 1723 (2010).
- <sup>14</sup>Y. Okawa, M. Nagano, S. Hirota, H. Kobayashi, T. Ohno, and M. Watanabe, *Biosens. Bioelectron.* **14**, 229 (1999).
- <sup>15</sup>L. Huang, H. Shen, M. Atkinson, and R. Kennedy, *Proc. Natl. Acad. Sci. USA* **92**, 9608 (1995).
- <sup>16</sup>S.-K. Jung, L. M. Kauri, W.-J. Qian, and R.T. Kennedy, *J. Bio. Chem.* **9**, 6642 (2000).
- <sup>17</sup>L. M. Kauri, S.-K. Jung, and R. T. Kennedy, *Biochem. Biophys. Res. Commun.* **304**, 371 (2003).
- <sup>18</sup>R. M. Wightman, *Science* **311**, 1570 (2006).
- <sup>19</sup>A. Schulte and W. Schuhmann, *Angew. Chem. Int. Ed.* **46**, 8760 (2007).
- <sup>20</sup>S. Isik and W. Schuhmann, *Angew. Chem. Int. Ed.* **45**, 7451 (2006).
- <sup>21</sup>S. Borgmann, I. Radtke, T. Erichsen, A. B. Priv.-Doz, R. Heumann, and W. Schuhmann, *ChemBiochem* **7**, 662 (2006).
- <sup>22</sup>S. Isik, L. Berdondini, J. Oni, A. Blöchl, M. Koudelka-Hep, and W. Schuhmann, *Biosens. Bioelectron.* **20**, 1566 (2005).
- <sup>23</sup>A. Revzin, R. Russell, V. Yadavalli, W-G Koh, C. Deister, D. Hile, M. Mellott, and M. Pishko, *Langmuir* **17**, 5440 (2001).
- <sup>24</sup>J. Y. Lee, S. S. Shah, J. Yan, M.C. Howland, A.N. Parikh, T. Pan, and A. Revzin, *Langmuir* **25**, 3880 (2009).
- <sup>25</sup>A. Revzin, R. G. Tompkins, and M. Toner, *Langmuir* **19**, 9855 (2003).
- <sup>26</sup>T. J. Ohara, R. Rajagopalan, and A. Heller, *Anal. Chem.* **66**, 2451 (1994).
- <sup>27</sup>W. G. Koh and M. Pishko, *Sens. Actuators B* **106**, 335 (2005).
- <sup>28</sup>J. Yan, V. Pedrosa, A. Simonian, and A. Revzin, *ACS Appl. Mat. Interfaces* **2**, 748 (2010).
- <sup>29</sup>C. A. P. Quinn, R. E. Connor, and A. Heller, *Biomaterials* **18**, 1665 (1997).
- <sup>30</sup>C. P. Quinn, C. P. Pathak, A. Heller, and J. Hubbell, *Biomaterials* **16**, 389 (1995).
- <sup>31</sup>H. Zhu, J. Yan, and A. Revzin, *Colloids Surf. B* **64**, 260 (2008).
- <sup>32</sup>H. Zhu, G. Stybayeva, M. Macal, E. Ramanculov, M. George, S. Dandekar, and A. Revzin, *Lab Chip* **8**, 2197 (2008).
- <sup>33</sup>C. Li, H. Zhang, P. Wu, Z. Gong, G. Xu, and C. Cai, *Analyst* **136**, 1116 (2011).
- <sup>34</sup>D. Chen, Q. Wang, J. Jin, P. Wu, H. Wang, S. Yu, H. Zhang, and C. Cai, *Anal. Chem.* **82**, 2448 (2010).
- <sup>35</sup>P. Du, B. Zhou, and C. X. Cai, *J. Electroanal. Chem.* **614**, 149 (2008).
- <sup>36</sup>M. Niculescu, C. Nistor, I. Frebort, P. Pe, B. Mattiasson, and E. Csöregi, *Anal. Chem.* **72**, 1591 (2000).
- <sup>37</sup>C. Ren, Y. Song, Z. Li, and G. Zhu, *Anal. Bioanal. Chem.* **381**, 1179 (2005).
- <sup>38</sup>H. P. Hartung and K. V. Toyka, *Eur. J. Pharmacol.* **89**, 301 (1983).
- <sup>39</sup>J. Yan, Y. Sun, H. Zhu, L. Marcu, and A. Revzin, *Biosens. Bioelectron.* **24**, 2604 (2009).
- <sup>40</sup>C. F. Nathan and R. K. Root, *J. Exp. Med.* **146**, 1648 (1977).
- <sup>41</sup>T. P. Szatrowski and C. F. Nathan, *Cancer Res.* **51**, 794 (1991).
- <sup>42</sup>P. A. Ward, R. E. Duque, M. C. Sulavik, and K. J. Johnson, *Am. J. Pathol.* **110**, 297 (1983).